



This discussion paper is/has been under review for the journal Geoscientific Model Development (GMD). Please refer to the corresponding final paper in GMD if available.

SEHR-ECHO v1.0: a Spatially-Explicit Hydrologic Response model for ecohydrologic applications

B. Schaeffli¹, L. Nicótina², C. Imfeld^{1,*}, P. Da Ronco^{1,3,**,***}, E. Bertuzzo¹, and A. Rinaldo^{1,3}

¹Laboratory of Ecohydrology, School of Architecture, Civil and Environmental Engineering, Ecole Polytechnique Fédérale de Lausanne, Switzerland

²Risk Management Solutions Ltd., London, UK

³Dipartimento di Ingegneria Civile, Edile e Ambientale Università di Padova, Padua, Italy

* now at: Hollinger Engineering, Ecublens, Switzerland

** now at: Impacts on Soil and Coasts Division, Euro-Mediterranean Center for Climate Change, Capua (CE), Italy

*** now at: Department of Civil and Environmental Engineering – Politecnico di Milano, Milano, Italy

Received: 28 January 2014 – Accepted: 8 March 2014 – Published: 19 March 2014

Correspondence to: B. Schaeffli (bettina.schaeffli@epfl.ch)

Published by Copernicus Publications on behalf of the European Geosciences Union.

Title Page

Abstract

Introduction

Conclusions

References

Tables

Figures



Back

Close

Full Screen / Esc

Printer-friendly Version

Interactive Discussion



Abstract

This paper presents the Spatially-Explicit Hydrologic Response (SEHR) model developed at the Laboratory of Ecohydrology of the Ecole Polytechnique Fédérale de Lausanne for the simulation of hydrological processes at the catchment scale. The key concept of the model is the formulation of water transport by geomorphologic travel time distributions through gravity-driven transitions among geomorphic states: the mobilization of water (and possibly dissolved solutes) is simulated at the sub-catchment scale and the resulting responses are convolved with the travel paths distribution within the river network to obtain the hydrologic response at the catchment outlet. The model thus breaks down the complexity of the hydrologic response into an explicit geomorphological combination of dominant spatial patterns of precipitation input and of hydrologic process controls. Nonstationarity and nonlinearity effects are tackled through soil moisture dynamics in the active soil layer. We present here the basic model set-up for precipitation–runoff simulation. The performance of the model is illustrated for a snow-dominated catchment in Switzerland with a small glacier cover.

1 Introduction

Hydrological processes result from natural processes that vary strongly in space, such as precipitation, evaporation or infiltration into the subsoil (McDonnell et al., 2007; Beven, 2012). Accordingly, most state-of-the art hydrologic response models have two fundamental components to describe the arrival of water and transported substances at a control section: a component to simulate the temporal evolution of water storage (and possibly of energy or of solutes) and released fluxes in some hydrologically meaningful sub-units and a component to describe the transport of the fluxes between the sub-units along the river network, (e.g. Hingray et al., 2010; Clark et al., 2008; Kunstmann and Stadler, 2005). There are, however, many models without an explicit description of the water flow within the landscape and the river network. This transport component is

GMDD

7, 1866–1904, 2014

The hydrologic
response model
SEHR-ECHO v1.0

B. Schaefli et al.

Title Page

Abstract

Introduction

Conclusions

References

Tables

Figures

⏪

⏩

◀

▶

Back

Close

Full Screen / Esc

Printer-friendly Version

Interactive Discussion



The hydrologic response model SEHR-ECHO v1.0

B. Schaefli et al.

Title Page

Abstract

Introduction

Conclusions

References

Tables

Figures

⏪

⏩

◀

▶

Back

Close

Full Screen / Esc

Printer-friendly Version

Interactive Discussion

either completely omitted as in lumped models (Perrin et al., 2003; Merz and Blöschl, 2004), assumed to be negligible at the spatio-temporal scale of interest (Viviroli et al., 2009; Schaefli et al., 2005), or assumed to fall out of the sum of transport processes simulated between small spatial units, without further parameterizing flow in channels (e.g. Tague and Band, 2001; Wigmosta et al., 1994; Liu and Todini, 2002).

Some models use an arbitrary (calibrated) discharge routing function to smooth the response computed at the scale of a (sub-)catchment, e.g. with a triangular function as in the HBV model (Bergström, 1995) and derivations thereof (Wrede et al., 2013; Das et al., 2008). Finally, there exist models that can be thought of as having an implicit routing component (Tague and Band, 2001) even if they are applied in a completely lumped manner, i.e. a component that accounts statistically for spatial differences of runoff generation, such as Hymod (Boyle, 2000; Moradkhani et al., 2005) or the well-known Topmodel with its topographical wetness index (Beven and Kirkby, 1979) (which is, however, generally not applied in a lumped manner).

Most existing catchment-scale model applications show an explicit parameterization of channeled flow only for the largest rivers in the analyzed system, for which typically a kinematic wave-based routing is used (e.g. Clark et al., 2008), assuming that at the sub-catchment level, the effect of travel times in channels are negligible at the considered spatio-temporal resolution. This might typically hold for hourly discharge simulation with sub-catchments of a few 10–100 km² in reasonably steep environments (e.g. Hingray et al., 2010).

Traditionally, the range of aforementioned hydrological models is classified into (semi-)lumped and (semi-)distributed (Reed et al., 2004; Beven, 2012), a classification which refers essentially to the parameterization of the temporal evolution of the water storage within the catchment. The terms *distributed* or *semi-distributed* (e.g. Das et al., 2008) generally refer to grid-based models or sub-catchment set-ups with different parameter sets for each spatial unit, whereas semi-lumped implies some degree of spatial discretization but with a single parameter set and generally without flow

routing through the landscape (e.g. Schaefli et al., 2005). Although not directly related, it is often implied that distributed models are more physics-based.

We propose the term of a spatially-explicit hydrologic response (SEHR) model for any model that explicitly parameterizes both, spatial patterns of water storage evolution as well as the effect of geomorphology on the travel time of water having different spatial origins.

Hereafter, we describe a simple catchment-scale hydrologic model developed at the Laboratory of Ecohydrology (ECHO) of the Ecole Polytechnique Fédérale de Lausanne, SEHR-ECHO, that explicitly accounts for the spatial variabilities in the runoff generation process and the heterogeneity of the flow-paths within the catchment. The model builds on the geomorphic theory of the hydrologic response (Rodriguez-Iturbe and Valdés, 1979; Rodriguez-Iturbe and Rinaldo, 1997; Rinaldo et al., 2006) pursuing an accurate description of riverine hydraulic processes through the use of the geomorphologic dispersion (Rinaldo et al., 1991), providing a general framework to formulate spatially-explicit models (e.g. Nicótina et al., 2008; Tobin et al., 2013). In such an approach, nonlinearities and nonstationarities of the hydrologic response (e.g. McDonnell et al., 2010; Botter et al., 2011; Sivapalan et al., 2002; Hrachowitz et al., 2013) are embedded in the parameterization of the soil moisture dynamics and the related dominant runoff generation processes at the source area scale.

The general model concept is introduced in Sect. 2 and implementation details discussed in Sect. 3. For illustration purposes, the model is applied to an example case study from Switzerland (Sect. 4), for which we discuss the discharge simulation performance in Sect. 5, before summarizing the main conclusions (Sect. 6).

2 Model description

The SEHR-ECHO model is composed of two main components (Fig. 1): (i) a precipitation–runoff transformation module that computes surface and sub-surface water fluxes from the source areas (the basic subunits that describe the spatial

The hydrologic response model SEHR-ECHO v1.0

B. Schaefli et al.

Title Page

Abstract

Introduction

Conclusions

References

Tables

Figures



Back

Close

Full Screen / Esc

Printer-friendly Version

Interactive Discussion



structure of the model domain), and (ii) a routing module that computes fluxes in the river network through to the control section (i.e. the outlet). In other terms, the model is composed of a module for unchanneled state processes at the source area scale and one for channeled state transport (Rinaldo et al., 2006).

5 The source areas are extracted from a digital elevation model (DEM) with the well-known Taudem algorithm (Tarboton, 1997) for subcatchment and river network delin-
10 eation (see Sect. 4 for further details). The scale of these source areas are selected such as to allow for sufficiently homogenous hydro-meteorological conditions without losing too much geomorphologic complexity. Relevant geomorphologic issues are dis-
cussed in (Rodriguez-Iturbe and Rinaldo, 1997).

2.1 Precipitation–runoff module at source area scale

The precipitation–runoff module solves the mass and energy balance equations at the source area scale. This component is driven by mass (i.e. precipitation) and energy (i.e. temperature) input time series, which need to be properly provided at the source
15 area scale. The choice of methods to interpolate the observed input time series to this scale depends on the variable (precipitation, temperature), on the application and on the simulation time step (e.g. Tobin et al., 2011), and the choice of the general method is largely independent of the exact set-up of the hydrological model. In the remainder
20 of this section we describe the precipitation–runoff transformation for one source area assuming the input variables are provided at the proper spatial and temporal scales.

The precipitation–runoff transformation module has the following key elements: inter-
ception and re-evaporation of intercepted water, rainfall-/snowfall separation, evolution
of water stored in the snowpack in solid form, evolution of the liquid water content
of the snowpack, equivalent precipitation (rain and meltwater)–runoff transformation. If
25 a source area has partial glacier cover, the runoff resulting from the glacier is computed separately (Fig. 1).

GMDD

7, 1865–1904, 2014

The hydrologic response model SEHR-ECHO v1.0

B. Schaefli et al.

Title Page

Abstract

Introduction

Conclusions

References

Tables

Figures

◀

▶

◀

▶

Back

Close

Full Screen / Esc

Printer-friendly Version

Interactive Discussion



Interception $I_c(t)$ is simulated using a constant interception capacity ρ :

$$I_c(t) = \min[\rho, P(t)], \quad (1)$$

where $P(t)$ [LT^{-1}] is the precipitation and ρ [LT^{-1}] is the maximum interception during a time step t (e.g. Fenicia et al., 2006). No separation between the aggregation state of precipitation (snow, rain) is made for ρ , a simplification which is not advisable for applications to catchments with important vegetation cover (e.g. Gelfan et al., 2004).

Part of intercepted water is assumed to re-evaporate during the same time step, limited by potential evaporation $E_{\text{pot}}(t)$ [LT^{-1}]:

$$E_i(t) = \min[E_{\text{pot}}(t), I_c(t)], \quad (2)$$

where $E_i(t)$ [LT^{-1}] is the evaporation flux from intercepted water. This evaporated water is assumed to not be available for the precipitation–runoff generation process, i.e. total incoming precipitation is reduced to net precipitation P_n [LT^{-1}]

$$P_n(t) = P(t) - E_i(t). \quad (3)$$

E_{pot} is reduced to potential transpiration $E_{\text{t,pot}}$ [LT^{-1}] by the amount of E_i :

$$E_{\text{t,pot}}(t) = E_{\text{pot}}(t) - E_i(t). \quad (4)$$

The estimation of the aggregation state of precipitation is based on a simple temperature threshold T_r [$^{\circ}\text{C}$] (Schaeffli et al., 2005) that splits net precipitation P_n into rainfall $P_r(t)$ [LT^{-1}] and snowfall $P_s(t)$ [LT^{-1}] depending on the mean temperature $T(t)$ (for a smooth threshold approach see Schaeffli and Huss, 2011).

The evolution of the water equivalent of the snowpack height h_s [L] is computed as:

$$\frac{dh_s}{dt} = P_s(t) - M_s(t) + F_s(t) - G_s(t), h_s > 0 \quad (5)$$

Title Page

Abstract

Introduction

Conclusions

References

Tables

Figures

⏪

⏩

◀

▶

Back

Close

Full Screen / Esc

Printer-friendly Version

Interactive Discussion



where $M_s(t)$ [LT^{-1}] is the snowmelt due to energy input from the atmosphere, $F_s(t)$ [LT^{-1}] is the flux of refreezing water during periods of negative heat input and $G_s(t)$ [LT^{-1}] is the snowmelt due to ground heat flux (all in water equivalent). G_s is assumed to be constant in time, $G_s = G_{\max}$ as long as there is a snowpack:

$$G_s(t) = \begin{cases} G_{\max} & \text{if } h_s(t) > 0 \\ 0 & \text{if } h_s(t) = 0 \end{cases} \quad (6)$$

The snowmelt M_s is modeled as linearly related to positive air temperature according to the temperature-index or degree-day approach (Hock, 2003):

$$M_s(t) = \begin{cases} a_s(T(t) - T_m) & \text{if } T(t) > T_m, h_s(t) > 0 \\ 0 & \text{otherwise} \end{cases} \quad (7)$$

where a_s is the degree-day factor for snow melt [$\text{LT}^{-1}\text{°C}^{-1}$], T_m [°C] is the threshold temperature for melting that is set to 0°C .

Refreezing F_s is assumed to occur when $T(t) < T_m$ and is linearly related to negative air temperature with a freezing degree-day factor that is proportional to, but smaller than the melt degree-day factor a_s (Kokkonen et al., 2006; Formetta et al., 2013):

$$F_s(t) = \begin{cases} a_f a_s (T_m - T(t)) & \text{if } T(t) < T_m, h_s(t) > 0 \\ 0 & \text{otherwise} \end{cases} \quad (8)$$

where $a_f \in [0, 1]$ is the degree-day reduction factor for refreezing.

The snowpack is assumed to have a certain water retention capacity $\theta \cdot h_s$ [mm] and water is released from the snowpack only if this retention capacity is exceeded. The balance equation for the liquid water h_w [L] content of the snowpack is written as:

$$\frac{dh_w}{dt} = P_r(t) + M_s(t) - F_s(t) - M_w(t), \quad (9)$$

The hydrologic response model SEHR-ECHO v1.0

B. Schaefli et al.

Title Page

Abstract

Introduction

Conclusions

References

Tables

Figures

⏪

⏩

◀

▶

Back

Close

Full Screen / Esc

Printer-friendly Version

Interactive Discussion



where the snowpack outflow M_w only occurs if the air temperature is above melting conditions and if the water retention capacity θ is reached:

$$M_w(t) = \begin{cases} P_r(t) + M_s(t) - F_s(t) & \text{if } h_w = \theta h_s \\ 0 & \text{if } h_w < \theta h_s \end{cases} \quad (10)$$

It is noteworthy that rainfall P_r only occurs if $T > T_r$, snowmelt M_s only if $T > T_m$ and refreezing F_s only if $T < T_m$. It generally holds that $T_r > T_m = 0^\circ\text{C}$ translating the well known fact that snowfall can occur at temperatures above the melt temperature (for an analysis of observed snowfall at the Davos station, see Rohrer et al., 1994). The general case of Eq. (10) holds for all values of the threshold parameters or for fuzzy transitions between rain- and snowfall.

The water fluxes P_r , G_s and M_w are summed up to produce the equivalent precipitation P_{eq} that enters the equivalent-precipitation–runoff transformation:

$$P_{eq}(t) = \begin{cases} P_r(t) & \text{if } h_s = 0 \\ G_s(t) + M_w(t) & \text{if } h_s > 0 \end{cases} \quad (11)$$

The partitioning of equivalent precipitation into surface runoff, fast and slow sub-surface runoff and transpiration resulting from water infiltration and percolation in the subsoil is performed via a minimalist description of the soil moisture dynamics at the source area scale (Laio et al., 2001; Rodriguez-Iturbe and Porporato, 2004; Rodriguez-Iturbe et al., 1999):

$$\eta Z_r \frac{ds(t)}{dt} = F_i(t) - E_t(t) - L(t), \quad 0 \leq s \leq 1 \quad (12)$$

where η [–] is the soil porosity, Z_r [L] is the depth of the soil layer that is active during water redistribution processes, s [–] is the relative soil moisture in the active layer, F_i [L T^{-1}] is the infiltration rate, E_t [L T^{-1}] is the rate of transpiration of water from the root

GMDD

7, 1865–1904, 2014

The hydrologic response model SEHR-ECHO v1.0

B. Schaefli et al.

Title Page

Abstract

Introduction

Conclusions

References

Tables

Figures

⏪

⏩

◀

▶

Back

Close

Full Screen / Esc

Printer-friendly Version

Interactive Discussion



zone and L [L T^{-1}] is the water flux (called leakage here) mobilized from the root zone as subsurface flow.

It is noteworthy that this soil moisture dynamics equation, if forced with Poisson infiltration, can be solved exactly for a number of cases and forms the basis of substantial analytic work on the probabilistic properties of stream flow (Botter et al., 2007b, a; Botter, 2010).

The leakage L is parameterized as a non-linear function of the soil moisture as:

$$L(t) = K_{\text{sat}} s(t)^c, \quad (13)$$

where K_{sat} [L T^{-1}] is the saturated hydraulic conductivity and c the Clapp–Hornberger exponent (Clapp and Hornberger, 1978).

The transpiration rate is a linear function of relative soil moisture between the wilting point, s_w [-] (i.e. the moisture content below which the plants cannot further extract water from the soil) and the upper limit of water stress, s_m [-], at which it is assumed to reach the limit imposed by the potential transpiration rate (e.g Porporato et al., 2004):

$$E_t(t) = \min \left[E_{t,\text{pot}} \frac{s - s_w}{s_m - s_w}, E_{t,\text{pot}} \right]. \quad (14)$$

The infiltrated water corresponds to the equivalent precipitation from which direct surface runoff is subtracted:

$$F_i(t) = P_{\text{eq}}(t) - R_{\text{hort}}(t) - R_{\text{dun}}(t), \quad (15)$$

where R_{hort} [L T^{-1}] is surface runoff occurring if the infiltration capacity is exceeded and R_{dun} [L T^{-1}] is surface runoff occurring if the source area is saturated. These two mechanisms of surface runoff, inspired from Hortonian and Dunne overland flow (e.g. Dingman, 2002), enable the model to simulate different times of reaction to a precipitation or melt water input.

The hydrologic response model SEHR-ECHO v1.0

B. Schaefli et al.

Title Page

Abstract

Introduction

Conclusions

References

Tables

Figures



Back

Close

Full Screen / Esc

Printer-friendly Version

Interactive Discussion



The hydrologic response model SEHR-ECHO v1.0

B. Schaefli et al.

Title Page

Abstract

Introduction

Conclusions

References

Tables

Figures

◀

▶

◀

▶

Back

Close

Full Screen / Esc

Printer-friendly Version

Interactive Discussion



R_{hort} is parameterized with a constant maximum infiltration capacity ϕ [LT^{-1}]:

$$R_{\text{hort}}(t) = \begin{cases} \max[P_{\text{eq}}(t) - \phi, 0] & \text{if } s(t) < 1 \\ 0 & \text{if } s(t) = 1 \end{cases} \quad (16)$$

where ϕ is supposed to be constant in time. If the soil is saturated, $s(t) = 1$, R_{dun} occurs

$$R_{\text{dun}}(t) = \begin{cases} P_{\text{eq}}(t) & \text{if } s(t) = 1 \\ 0 & \text{if } s(t) < 1 \end{cases} \quad (17)$$

The water mobilized from the active layer L is transformed to subsurface runoff at the source area outlet through two linear reservoirs that simulate a fast and a slow subsurface flux, R_{fast} [LT^{-1}] and R_{slow} [LT^{-1}] (similar to the e.g. the formulation in the HBV model Bergström, 1995). The part of L feeding the slow subsurface flux, L_{slow} , is assumed to be a constant flux L_{max} limited by L :

$$L_{\text{slow}}(t) = \min[L(t), L_{\text{max}}]. \quad (18)$$

The linear reservoir equations for the fast and slow subsurface runoff thus read as:

$$\frac{dS_{\text{fast}}}{dt} = L(t) - L_{\text{slow}}(t) - R_{\text{fast}}(t), \quad (19)$$

$$\frac{dS_{\text{slow}}}{dt} = L_{\text{slow}}(t) - R_{\text{slow}}(t). \quad (20)$$

where S_{fast} [L] and S_{slow} [L] are the water storage in the fast and the slow reservoirs. R_{fast} [LT^{-1}] and R_{slow} [LT^{-1}] are the fast and slow reservoir outflows, which are supposed to linearly depend on the storage, i.e. $R_{\text{fast}} = k_{\text{fast}} S_{\text{fast}}$ and $R_{\text{slow}} = k_{\text{slow}} S_{\text{slow}}$ where k_{fast}^{-1} [T] and k_{slow}^{-1} [T] are the mean residence times.

Note that s is a relative soil moisture, whereas S_{slow} and S_{fast} have length units.

2.2 Discharge simulation from glacierized subcatchments

If a source area has a partial glacier coverage, ice is assumed to start melting if $h_s = 0$ (Schaeffli et al., 2005):

$$M_i = \begin{cases} a_i (T(t) - T_m) & \text{if } T(t) > T_m, h_s(t) = 0 \\ 0 & \text{otherwise} \end{cases} \quad (21)$$

5 where a_i [$\text{LT}^{-1} \text{°C}^{-1}$] is the degree-day factor for ice melt. This melt is routed to the subcatchment outlet through a linear reservoir with coefficient k_{ice} . The routing to the catchment outlet follows the general procedure (see hereafter) but the flux is weighted according to the fraction of source area that is glacier covered. No glacier surface dynamics are modelled (e.g Huss et al., 2010), the glacier cover is assumed to be
10 constant (but it can of course be updated for different simulation periods).

2.3 Discharge simulation at catchment outlet

The transport of the runoff components through the river network uses a linear approach, assuming that most relevant nonlinear processes are captured through the source area-scale precipitation–runoff transformation. The total discharge at the catchment outlet is obtained by convolution of each of the fluxes R (surface runoffs R_{hprt} ,
15 R_{dun} , subsurface runoffs R_{fast} , R_{slow} and ice melt runoff R_{ice}) from all source areas with a travel time distribution $f_\gamma(t)$ along its flow path γ to the catchment outlet (Fig. 2).

The probability density functions of travel times, $f_\gamma(t)$ (assumed statistically independent) are obtained from the travel time distributions in all channels $C_j \rightarrow C_k \rightarrow C_\Omega$
20 composing them (Gupta et al., 1980; Rinaldo et al., 1991):

$$f_\gamma(t) = f_{C_j}(t) * f_{C_k}(t) * \dots * f_\Omega(t) \quad (22)$$

where $*$ is the convolution operator and Ω is the outlet. For the example illustrated in Fig. 2, the travel path from the source area A_1 to the outlet is made up of two collecting channels C_1 and C_3 .

Title Page

Abstract

Introduction

Conclusions

References

Tables

Figures

◀

▶

◀

▶

Back

Close

Full Screen / Esc

Printer-friendly Version

Interactive Discussion



The travel time distributions within channeled states C_j are obtained assuming longitudinal 1-D dispersion, which is a reasonable assumption for open channel flow in low order rivers (Rinaldo et al., 1991):

$$f_{C_j}(t) = \frac{1}{4(\pi D_\ell t^3)^{(1/2)}} \ell_j \exp \left\{ - \left[\frac{(\ell_j - vt)^2}{4D_\ell t} \right] \right\}, \quad (23)$$

5 where D_ℓ [$L^2 T^{-1}$] is the hydrodynamic dispersion coefficient, ℓ_j [L] is the channel length and v [$L T^{-1}$] is the average velocity.

The simulated discharge at the catchment outlet becomes

$$Q = Q_{\text{fast}} + Q_{\text{slow}} + Q_{\text{hort}} + Q_{\text{dun}} + Q_{\text{ice}}, \quad (24)$$

where each of the discharge components Q_{xyz} equals

$$10 \quad Q_{xyz} = \sum_{\gamma=1}^n [R_{xyz,\gamma}(t) * f_\gamma(t)]. \quad (25)$$

3 Model implementation

The model requires temperature, precipitation and potential evaporation time series for each subcatchment and, for model calibration, at least one concomitant discharge time series observed at the catchment outlet. The numerical implementation uses a fixed
15 time step and a 4th order Runge–Kutta scheme to compute the soil moisture evolution. The other stores (fast and slow subsurface flux stores, solid and liquid snow stores) are solved with explicit time-stepping, which is justified given that these stores have only one outflux, linearly dependent on the storage.

The provided code (see Supplement) is developed in Matlab R2010b. The parameterization of each of the presented hydrological processes can easily be modified.
20

The basic model structure (passing of variables and parameters among functions) has been designed for an easy combination with the now widely used optimization algorithms developed by Vrugt et al. (2003, 2009). For the example presented in this paper, the model is, however, calibrated with simple Monte Carlo generation within a priori parameter ranges (details in Sect. 4).

3.1 Identification of model parameter patterns

The physical parameters of SEHR-ECHO, which describe the physiographic catchment characteristics and can be extracted from topographic data, are listed in Table 1. The model parameters that require calibration or a relevant method of a priori estimation are summarized in Table 2 (along with a range of a priori values). Depending on the application, all these parameters might be made variable in space, especially the ones for which there are known spatial patterns.

It is, in particular, recommended to relate the mean residence time k_{fast}^{-1} of subcatchment-scale subsurface fluxes to the source area A_Y as:

$$\frac{1}{k_{\text{fast},Y}} \sim A_Y^\xi, \quad (26)$$

where the scaling coefficient ξ can be set to values of around 1/3 (Alexander, 1972; Pilgrim et al., 1982). In practical terms, such a scaling for k_{fast} is obtained by calibrating a generic reservoir coefficient k_{cal} such that

$$\frac{1}{k_{\text{fast},Y}} = \frac{1}{k_{\text{cal}}} \left(\frac{A_Y}{\langle A_Y \rangle} \right)^\xi, \quad (27)$$

where $\langle A_Y \rangle$ is the mean subcatchment area. The coefficient k_{slow} is then related to k_{fast} through the calibration of a multiplication parameter m_k such that

$$\frac{1}{k_{\text{slow},Y}} = m_k \frac{1}{k_{\text{fast},Y}}. \quad (28)$$

Title Page

Abstract

Introduction

Conclusions

References

Tables

Figures

◀

▶

◀

▶

Back

Close

Full Screen / Esc

Printer-friendly Version

Interactive Discussion



It might be tempting to derive the spatial variability of the active soil depth from soil production theory (Heimsath et al., 1997). Such an approach might e.g. assume that the soil depth of a source area is proportional to the mean topographic curvature in topographically convex areas. Another idea could be to identify topographically concave areas that can be assumed to be saturated at all times. For applications similar to the one presented here, different model tests showed, however, that the effect of spatially variable soil depth on simulated discharge can be compensated by the other model parameters (Nicótina et al., 2011); this approach is therefore not further pursued here.

The saturated hydraulic conductivity can easily be distributed in space according to observed land use and soil types; an example is discussed in Sect. 4 for the present case study. Imposing additional spatial parameter patterns related to directly observable physiographic characteristics is readily possible, but beyond the scopes of the present work.

4 Case study

The Dischmabach catchment, located in the south-east of Switzerland near Davos (Fig. 3), has a size of 43.3 km² at the Kriegsmatten gauging station, for which long discharge time series are available from the Swiss Federal Office for the Environment. Its elevation ranges from 1668 m a.s.l. up to 3146 m a.s.l. (mean altitude 2372 m a.s.l.) with around 2.1 % of the catchment area covered by glaciers. The annual mean temperature at mean elevation is around -0.5 °C. The discharge regime shows a strong seasonal pattern due to accumulation and melting of snow. The relatively steep hillslopes are covered with pasture (38 %) and forest (10 %); around 16 % of the catchment are bare soil, rock outcrops cover 24 % (Verbunt et al., 2003). The geology is crystalline composed of gneiss and amphibolites, overlain by shallow soils (Verbunt et al., 2003). The nearby meteorological station of Weissfluhjoch (2690 m a.s.l.) records around 1450 mm year⁻¹ of precipitation (period 1981–1999), which is relatively low compared to other Alpine locations at the same altitude. The discharge over the same

The hydrologic response model SEHR-ECHO v1.0

B. Schaefli et al.

Title Page

Abstract

Introduction

Conclusions

References

Tables

Figures



Back

Close

Full Screen / Esc

Printer-friendly Version

Interactive Discussion



period was around $1350 \text{ mm year}^{-1}$. The mean evaporation in this catchment is around 300 mm year^{-1} for the period 1973–1992 (Menzel et al., 1999). Part of the discharge is due to net glacier ice melt.

The subcatchments as well as the river network characteristics required to run the model (network topology, river reach lengths) are identified with TauDEM Version 5 (Tarboton, 1997), a hydrologic terrain analysis tool which is freely available under the terms of the GNU General Public License version 2 at <http://hydrology.usu.edu/taudem/taudem5/>. The 23 subcatchments as well as the river network are shown (Fig. 3).

The temperature time series for each subcatchment is obtained through a linear interpolation of the temperature observed at the Davos weather station (1594 m a.s.l.) to the mean subcatchment altitude, using the average temperature lapse rate between this and the Weissfluhjoch station (which equals $-0.50 \text{ }^\circ\text{C}/100 \text{ m}$). The precipitation for each subcatchment is the one recorded at Weissfluhjoch. The potential evaporation is evaluated with the Priestley–Taylor method (Maidment, 1993; Priestley and Taylor, 1972) using the Weissfluhjoch meteorological data.

Given the important heterogeneity of land use in this catchment, we distribute the saturated hydraulic conductivity according to land use types, which are available from the Swiss land use data-based at a resolution of 100 m (Swiss Federal Office for Statistics, 2001). We assign each relevant land use class j a surface runoff coefficient r_j (see Supplementa, Table 1). Based on the distribution of r_j within each subcatchment γ , we compute the following scaling parameter

$$q_\gamma = \frac{\sum_j r_j f_j}{r_D}, \quad (29)$$

where γ identifies a given subcatchment, f_j is the relative frequency of occurrence of the land use class j within the subcatchment and r_D is the dominant land use class.

For each subcatchment, the saturated hydraulic conductivity is then obtained as

$$K_{\text{sat},\gamma} = q_\gamma K_{\text{sat}}, \quad (30)$$

GMDD

7, 1865–1904, 2014

The hydrologic response model SEHR-ECHO v1.0

B. Schaefli et al.

Title Page

Abstract

Introduction

Conclusions

References

Tables

Figures

⏪

⏩

◀

▶

Back

Close

Full Screen / Esc

Printer-friendly Version

Interactive Discussion



where k_y is the k th time step of year y and Y the total number of years. For the observed discharge of the Dischmabach, $N(Q_b)$ equals 0.74 at the daily time step and 0.73 at the hourly time step. For $N_L(Q_b)$ the values of the benchmark is 0.87 for the daily and the hourly time step.

Given the insignificant role of Horton direct runoff in this environment, this runoff mechanism is deactivated here (assuming infinite infiltration capacity). For all other processes, the a priori parameter ranges are obtained based on existing literature (see Table 2). The upper limit of the percolation flux feeding the slow subsurface flux, L_{\max} , is chosen equal to the mean daily precipitation. The upper limit of the average root zone depth is fixed to 1.5 m, which is a conservative estimate given the type of vegetation present. The generic fast subsurface residence time, k_{cal} , Eq. (27), is assumed to be of the order of magnitude of days and the slow subsurface residence to be substantially longer (maximum scaling factor $m_k = 50$).

A similar scaling approach is also used to ensure that the degree-day factor for ice a_i is higher than the one for snow a_s and that the retention capacity s_m is higher than the wilting point s_w .

5 Results

The calibration parameters of the SEHR-ECHO model have been estimated through simple Monte Carlo simulation for the Dischma catchment to illustrate the main features of this spatially-explicit model. Figure 4 shows the discharge simulation along with the simulated series of evapotranspiration and observed meteorological time series at the catchment outlet for the best NSE parameter set obtained with 35 000 parameter sets sampled uniformly within the prior distributions of Table 2. With a NSE value of 0.82 during calibration, this parameter set performs better than the benchmark model (Sect. 4). It furthermore gives reasonable estimates for evapotranspiration, which indicates that the observed precipitation time series is an acceptable proxy for catchment-scale area-average precipitation input.

GMDD

7, 1865–1904, 2014

The hydrologic response model SEHR-ECHO v1.0

B. Schaefli et al.

Title Page

Abstract

Introduction

Conclusions

References

Tables

Figures

⏪

⏩

◀

▶

Back

Close

Full Screen / Esc

Printer-friendly Version

Interactive Discussion



The hydrologic response model SEHR-ECHO v1.0

B. Schaefli et al.

Title Page

Abstract

Introduction

Conclusions

References

Tables

Figures



Back

Close

Full Screen / Esc

Printer-friendly Version

Interactive Discussion



The splitting between the three hillslope scale runoff generation processes corresponds to the expected pattern, without having been imposed during calibration: Fig. 5 illustrates that the slow subsurface component contributes essentially to base flow and that the direct surface runoff is activated only occasionally. (The corresponding sub-catchment scale state variables are given in Fig. 1 of the Supplement along with an example of the simulated snowpack evolution, Fig. 2.)

This parameter set comes along with a number of sets that lead to equally good discharge simulations for the reference performance criteria for the calibration period. The plots of NSE vs. NSE-log and of NSE vs. the relative bias (Fig. 6) illustrate that these performance criteria can be well optimized simultaneously, which is not always the case for hydrological models. Such models typically show a strong tradeoff between NSE and NSE-log because the same set of processes cannot reproduce high flows and recessions. This problem is reduced in the analyzed hydrologic regime where low flows are dominated by the long winter recession, relatively simple to simulate (see also the log discharge plot in Fig. 4).

A notable aspect of this SEHR-Echo application is that a large number of the best performing parameter sets at the daily time step perform equally well during the calibration period (1981–1992) and the validation period (1993–2000) and at the hourly time step (Fig. 6). This is also illustrated in Fig. 7 that shows the ensemble of discharge simulations obtained for the 100 best daily parameter sets (see Fig. 8) applied at the daily and the hourly simulation time step. The corresponding prediction limits span the observed discharge equally well at both time steps. The simulation bias increases however at the hourly time step (Table 3): this is most likely due to the assumption of a constant within-day relation between air temperature and snowmelt and refreezing and ice melt; the related parameters might require a specific calibration to the hourly time step or a more appropriate formulation for the hourly time step (Tobin et al., 2013).

The above evidence, time-scale independence and splitting between the runoff generation processes, are important hints that the model works well for the right reasons: the parameters play the role they have been designed for, rather than trying to mimic

omitted runoff generation processes or to compensate for the lack of spatial differentiation of travel times, which might typically occur for lumped models.

This conclusion is also supported by the good identifiability of some of the model key parameters, illustrated by the relatively peaky distributions in Fig. 8, which shows histograms of the best 100 parameter sets (in terms of NSE) at the daily time step. Albeit not providing a formal assessment of model and parameter uncertainty, this simple analysis illustrates that the model has a relatively well defined range of optimal parameters, which might be further refined for real-world applications and specific questions (e.g. extreme event analysis). It is noteworthy, however, that a flat distribution of the best performing parameter sets for a given specific parameter (e.g. here the wilting point) does not point towards model insensitivity with respect to this parameter, since its relation to other parameters might simply not be visible in the marginal distribution (Bardossy, 2007).

The question arises in as far the geomorphology-based set-up and the routing scheme influence the results. The model simulations are insensitive to hydrodynamic dispersion since its effect is overruled by advection. Given the relatively short distances in this catchment (the longest travel paths from a subcatchment to the outlet is 11 km), the velocity of in-stream discharge routing has only a minor effect at the daily time scale and a notable influence of the velocity on the simulated discharge would be obtained only with unrealistically low velocities (e.g. Yochum et al., 2012) (Fig. 9). For the hourly time step, any variation of flow velocity affects the discharge simulation and including this parameter in the calibration process might be a possible option, keeping in mind, however, that it might interact namely with the recession coefficients.

5.1 Comparison of the subcatchment set-up to elevation bands

Comparable precipitation–runoff models often either use a grid-based spatial discretization (e.g. Huss et al., 2008) or an elevation band approach (e.g. Schaeffli et al., 2005; Stahl et al., 2008) to account for temperature gradients as the strongest spatially-variable driver. Such an approach can be assumed to yield a more reliable

GMDD

7, 1865–1904, 2014

The hydrologic response model SEHR-ECHO v1.0

B. Schaeffli et al.

Title Page

Abstract

Introduction

Conclusions

References

Tables

Figures



Back

Close

Full Screen / Esc

Printer-friendly Version

Interactive Discussion



The hydrologic response model SEHR-ECHO v1.0

B. Schaefli et al.

Title Page

Abstract

Introduction

Conclusions

References

Tables

Figures

◀

▶

◀

▶

Back

Close

Full Screen / Esc

Printer-friendly Version

Interactive Discussion



representation of the snow accumulation and melt processes but it necessarily leads to a description of the equivalent precipitation–runoff transformation that cannot properly account for the spatial origin of flow. We compared the performance of a model set-up where the catchment is subdivided into 10 elevation bands (Fig. 3) to the subcatchment based set-up. A look on the model performance in terms of NSE and NSE-log for both set-ups (Fig. 10, top left) demonstrates that the elevation band approach marginally outperforms the subcatchment approach for the calibration period at the daily time step. If the best 100 of these parameter sets (in terms of NSE efficiency) are applied to the hourly time step (Fig. 10, top row, center column), the elevation band set-up does a noticeably better job. This higher performance however disappears for the validation period (Fig. 10, top right), which is a strong hint of overfitting during the calibration period, where the calibration parameters might compensate for the lack of a proper accounting for the spatial origin of flows.

This hypothesis is supported by the fact that if we use subcatchments divided into elevation bands, we obtain a consistent improvement of the discharge simulation performance at the hourly time step for the calibration and the validation period (Fig. 10, bottom row).

6 Conclusions

This paper presents a spatially-explicit precipitation–runoff model that formulates the hydrologic response of a catchment as a convolution of the subcatchment-scale hydrologic flow processes with the river network, where the kernels account for the spatial arrangements of the subcatchments linked by the river network. The hydrologic response accommodates directly any direct information on observable physiographic catchment characteristics such as in-stream flow paths lengths or subcatchment area as a proxy for subsurface residence time scaling. Remaining model parameters are calibrated on observed discharge. This spatially-explicit parameterization confers the model a unique transferability across time-scales, as has been demonstrated in this

paper based on a cryosphere-dominated catchment from the Swiss Alps where, due to the steep topography, travel times in unchanneled areas are dominating in-stream travel times. The main focus of this paper was on discharge simulation. Including appropriate formulations of subcatchment-scale mass transformation processes, the presented model can easily be extended to transport processes.

The Matlab version of the model will be available on <http://www.mathworks.ch/matlabcentral/fileexchange/>.

Supplementary material related to this article is available online at <http://www.geosci-model-dev-discuss.net/7/1865/2014/gmdd-7-1865-2014-supplement.zip>.

Acknowledgements. The research of the first author of this paper has been funded through an Ambizione grant of the Swiss National Science Foundation, SNSF, number PZ00P2_147366. The last author acknowledges funding from the ERC Advanced Grant RINEC 22761 and the SNSF grant 200021_135241. The meteorological data was obtained from MeteoSwiss and the discharge data from the Swiss Federal Office for the Environment.

References

- Alexander, G. N.: Effect of catchment area on flood magnitude, *J. Hydrol.*, 16, 225–240, doi:10.1016/0022-1694(72)90054-6, 1972. 1877
- Bárdossy, A.: Calibration of hydrological model parameters for ungauged catchments, *Hydrol. Earth Syst. Sci.*, 11, 703–710, doi:10.5194/hess-11-703-2007, 2007. 1883
- Bergström, S.: The HBV model, in: *Computer Models of Watershed Hydrology*, edited by: Singh, V. P., Water Resources Publications, Littleton, 443–476, 1995. 1867, 1874
- Beven, K.: *Rainfall–Runoff Modelling – the Primer*, 2nd edn., Wiley-Blackwell, Oxford, 2012. 1866, 1867
- Beven, K. and Kirkby, M.: A physically based, variable contributing area model of basin hydrology, *Hydrological Sciences Bulletin*, 24, 43–69, 1979. 1867

Title Page

Abstract

Introduction

Conclusions

References

Tables

Figures

◀

▶

◀

▶

Back

Close

Full Screen / Esc

Printer-friendly Version

Interactive Discussion



The hydrologic response model SEHR-ECHO v1.0

B. Schaefli et al.

Title Page

Abstract

Introduction

Conclusions

References

Tables

Figures

◀

▶

◀

▶

Back

Close

Full Screen / Esc

Printer-friendly Version

Interactive Discussion



- Botter, G.: Stochastic recession rates and the probabilistic structure of stream flows, *Water Resour. Res.*, 46, W12527, doi:10.1029/2010WR009217, 2010. 1873
- Botter, G., Porporato, A., Daly, E., Rodriguez-Iturbe, I., and Rinaldo, A.: Probabilistic characterization of base flows in river basins: roles of soil, vegetation, and geomorphology, *Water Resour. Res.*, 43, W06404, doi:10.1029/2006wr005397, 2007a. 1873
- Botter, G., Porporato, A., Rodriguez-Iturbe, I., and Rinaldo, A.: Basin-scale soil moisture dynamics and the probabilistic characterization of carrier hydrologic flows: slow, leaching-prone components of the hydrologic response, *Water Resour. Res.*, 43, W02417, doi:10.1029/2006wr005043, 2007b. 1873
- Botter, G., Bertuzzo, E., and Rinaldo, A.: Catchment residence and travel time distributions: the master equation, *Geophys. Res. Lett.*, 38, L11403, doi:10.1029/2011gl047666, 2011. 1868
- Boyle, D. P.: Multicriteria Calibration of Hydrological Models, Ph. D. thesis, University of Arizona, 2000. 1867
- Bras, R. and Rodriguez-Iturbe, I.: *Random Functions and Hydrology*, Addison Wesley, Reading, 1985. 1896
- Clapp, R. B. and Hornberger, G. M.: Empirical equations for some soil hydraulic-properties, *Water Resour. Res.*, 14, 601–604, doi:10.1029/WR014i004p00601, 1978. 1873, 1893
- Clark, M. P., Rupp, D. E., Woods, R. A., Zheng, X., Ibbitt, R. P., Slater, A. G., Schmidt, J., and Uddstrom, M. J.: Hydrological data assimilation with the ensemble Kalman filter: use of streamflow observations to update states in a distributed hydrological model, *Adv. Water Resour.*, 31, 1309–1324, doi:10.1016/j.advwatres.2008.06.005, 2008. 1866, 1867
- Comiti, F., Mao, L., Wilcox, A., Wohl, E. E., and Lenzi, M. A.: Field-derived relationships for flow velocity and resistance in high-gradient streams, *J. Hydrol.*, 340, 48–62, doi:10.1016/j.jhydrol.2007.03.021, 2007. 1893
- Das, T., Bardossy, A., Zehe, E., and He, Y.: Comparison of conceptual model performance using different representations of spatial variability, *J. Hydrol.*, 356, 106–118, doi:10.1016/j.jhydrol.2008.04.008, 2008. 1867
- Dingman, S.: *Physical Hydrology*, 2nd Edn., Prentice-Hall, Upper Saddle River, New Jersey, 2002. 1873, 1893
- Fenicia, F., Savenije, H. H. G., Matgen, P., and Pfister, L.: Is the groundwater reservoir linear? Learning from data in hydrological modelling, *Hydrol. Earth Syst. Sci.*, 10, 139–150, doi:10.5194/hess-10-139-2006, 2006. 1870

The hydrologic response model SEHR-ECHO v1.0

B. Schaefli et al.

Title Page

Abstract

Introduction

Conclusions

References

Tables

Figures

◀

▶

◀

▶

Back

Close

Full Screen / Esc

Printer-friendly Version

Interactive Discussion



Formetta, G., Kampf, S. K., David, O., and Rigon, R.: The Cache la Poudre river basin snow water equivalent modeling with NewAge-JGrass, *Geosci. Model Dev. Discuss.*, 6, 4447–4474, doi:10.5194/gmdd-6-4447-2013, 2013. 1871

Gelfan, A. N., Pomeroy, J. W., and Kuchment, L. S.: Modeling forest cover influences on snow accumulation, sublimation, and melt, *J. Hydrometeorol.*, 5, 785–803, doi:10.1175/1525-7541(2004)005<0785:mfcios>2.0.co;2, 2004. 1870

Gerrits, A. M. J., Pfister, L., and Savenije, H. H. G.: Spatial and temporal variability of canopy and forest floor interception in a beech forest, *Hydrol. Process.*, 24, 3011–3025, doi:10.1002/hyp.7712, 2010. 1893

Gupta, V. K., Waymire, E., and Wang, C. T.: A representation of an instantaneous unit-hydrograph from geomorphology, *Water Resour. Res.*, 16, 855–862, doi:10.1029/WR016i005p00855, 1980. 1875

Heimsath, A. M., Dietrich, W. E., Nishiizumi, K., and Finkel, R. C.: The soil production function and landscape equilibrium, *Nature*, 388, 358–361, doi:10.1038/41056, 1997. 1878

Hingray, B., Schaefli, B., Mezghani, A., and Hamdi, Y.: Signature-based model calibration for hydrologic prediction in mesoscale Alpine catchments, *Hydrolog. Sci. J.*, 55, 1002–1016, doi:10.1080/02626667.2010.505572, 2010. 1866, 1867

Hock, R.: Temperature index melt modelling in mountain areas, *J. Hydrol.*, 282, 104–115, doi:10.1016/S0022-1694(03)00257-9, 2003. 1871

Hrachowitz, M., Savenije, H., Bogaard, T. A., Tetzlaff, D., and Soulsby, C.: What can flux tracking teach us about water age distribution patterns and their temporal dynamics?, *Hydrol. Earth Syst. Sci.*, 17, 533–564, doi:10.5194/hess-17-533-2013, 2013. 1868

Huss, M., Farinotti, D., Bauder, A., and Funk, M.: Modelling runoff from highly glacierized alpine drainage basins in a changing climate, *Hydrol. Process.*, 22, 3888–3902, doi:10.1002/hyp.7055, 2008. 1883

Huss, M., Jouvét, G., Farinotti, D., and Bauder, A.: Future high-mountain hydrology: a new parameterization of glacier retreat, *Hydrol. Earth Syst. Sci.*, 14, 815–829, doi:10.5194/hess-14-815-2010, 2010. 1875

Kokkonen, T., Koivusalo, H., Jakeman, T., and Norton, J.: Construction of a degree-day snow model in the light of the ten iterative steps in model development, in: *Proceedings of the iEMSs Third Biennial Meeting: Summit on Environmental Modelling Software Society*, Burlington, USA, 4452–4454, 2006. 1871, 1893

The hydrologic response model SEHR-ECHO v1.0

B. Schaefli et al.

Title Page

Abstract

Introduction

Conclusions

References

Tables

Figures

◀

▶

◀

▶

Back

Close

Full Screen / Esc

Printer-friendly Version

Interactive Discussion



Kunstmann, H. and Stadler, C.: High resolution distributed atmospheric-hydrological modelling for Alpine catchments, *J. Hydrol.*, 314, 105–124, doi:10.1016/j.jhydrol.2005.03.033, 2005. 1866

Laio, F., Porporato, A., Ridolfi, L., and Rodriguez-Iturbe, I.: Plants in water-controlled ecosystems: active role in hydrologic processes and response to water stress – II. Probabilistic soil moisture dynamics, *Adv. Water Resour.*, 24, 707–723, doi:10.1016/s0309-1708(01)00005-7, 2001. 1872

Liu, Z. and Todini, E.: Towards a comprehensive physically-based rainfall–runoff model, *Hydrol. Earth Syst. Sci.*, 6, 859–881, doi:10.5194/hess-6-859-2002, 2002. 1867

Maidment, D. R. (Ed.): *Handbook of Hydrology*, McGraw-Hill, New York, 1993. 1879

McDonnell, J., Sivapalan, M., Vaché, K., Dunn, S., Grant, G., Haggerty, R., Hinz, C., Hooper, R., Kirchner, K., Roderick, M. L., Selker, J., and Weiler, M.: Moving beyond heterogeneity and process complexity: a new vision for watershed hydrology, *Water Resour. Res.*, 43, W07301, doi:10.1029/2006WR005467, 2007. 1866

McDonnell, J. J., McGuire, K., Aggarwal, P., Beven, K. J., Biondi, D., Destouni, G., Dunn, S., James, A., Kirchner, J., Kraft, P., Lyon, S., Maloszewski, P., Newman, B., Pfister, L., Rinaldo, A., Rodhe, A., Sayama, T., Seibert, J., Solomon, K., Soulsby, C., Stewart, M., Tetzlaff, D., Tobin, C., Troch, P., Weiler, M., Western, A., Wörman, A., and Wrede, S.: How old is streamwater? Open questions in catchment transit time conceptualization, modelling and analysis, *Hydrol. Process.*, 24, 1745–1754, doi:10.1002/hyp.7796, 2010. 1868

Menzel, L., Lang, H., and Rohmann, M.: Mean annual actual evaporation 1973–1992, in: *Hydrological Atlas of Switzerland*, Plate 4.1, Service Hydrologique et Géologique National, Bern, 1999. 1879

Merz, R. and Blöschl, G.: Regionalisation of catchment model parameters, *J. Hydrol.*, 95–123, 2004. 1867

Moradkhani, H., Hsu, K.-L., Gupta, H., and Sorooshian, S.: Uncertainty assessment of hydrologic model states and parameters: sequential data assimilation using the particle filter, *Water Resour. Res.*, 41, W05012, doi:10.1029/2004WR003604, 2005. 1867

Nash, J. E. and Sutcliffe, J. V.: River flow forecasting through conceptual models. Part I, a discussion of principles, *J. Hydrol.*, 10, 282–290, doi:10.1016/0022-1694(70)90255-6, 1970. 1880

The hydrologic response model SEHR-ECHO v1.0

B. Schaefli et al.

Title Page

Abstract

Introduction

Conclusions

References

Tables

Figures

◀

▶

◀

▶

Back

Close

Full Screen / Esc

Printer-friendly Version

Interactive Discussion



Nicótina, L., Alessi Celegon, E., Rinaldo, A., and Marani, M.: On the impact of rainfall patterns on the hydrologic response, *Water Resour. Res.*, 44, W12401, doi:10.1029/2007WR006654, 2008. 1868

Nicótina, L., Tarboton, D., Tesfa, T., and Rinaldo, A.: Hydrologic controls on equilibrium soil depths, *Water Resour. Res.*, 47, W04517, doi:10.1029/2010WR009538, 2011. 1878

Perrin, C., Michel, C., and Andreassian, V.: Improvement of a parsimonious model for stream-flow simulation, *J. Hydrol.*, 279, 275–289, 2003. 1867

Pilgrim, D. H., Cordery, I., and Baron, B. C.: Effects of catchment size on runoff relationships, *J. Hydrol.*, 58, 205–221, doi:10.1016/0022-1694(82)90035-X, 1982. 1877

Pomeroy, J. W., Gray, D. M., Shook, K. R., Toth, B., Essery, R. L. H., Pietroniro, A., and Hedstrom, N.: An evaluation of snow accumulation and ablation processes for land surface modelling, *Hydrol. Process.*, 12, 2339–2367, 1998. 1893

Porporato, A., Daly, E., and Rodriguez-Iturbe, I.: Soil water balance and ecosystem response to climate change, *Am. Nat.*, 164, 625–632, doi:10.1086/424970, 2004. 1873

Priestley, C. and Taylor, R.: On the assessment of surface heat flux and evaporation using large-scale parameters, *Mon. Weather Rev.*, 100, 81–92, doi:10.1175/1520-0493(1972)100<0081:OTAOSH>2.3.CO;2, 1972. 1879

Reed, S., Koren, V., Smith, M., Zhang, Z., Moreda, F., Seo, D.-J., and Participants, D.: Overall distributed model intercomparison project results, *J. Hydrol.*, 298, 27–60, doi:10.1016/j.jhydrol.2004.03.031, 2004. 1867

Rinaldo, A., Marani, M., and Rigon, R.: Geomorphological dispersion, *Water Resour. Res.*, 27, 513–525, 1991. 1868, 1875, 1876

Rinaldo, A., Botter, G., Bertuzzo, E., Uccelli, A., Settin, T., and Marani, M.: Transport at basin scales: 1. Theoretical framework, *Hydrol. Earth Syst. Sci.*, 10, 19–29, doi:10.5194/hess-10-19-2006, 2006. 1868, 1869

Rodriguez-Iturbe, I. and Porporato, A.: *Ecohydrology of Water-Controlled Ecosystems – Soil Moisture and Plant Dynamics*, Cambridge University Press, Cambridge, 2004. 1872

Rodriguez-Iturbe, I. and Rinaldo, A.: *Fractal River Basins: Chance and Self-Organization*, Cambridge University Press, New York, 1997. 1868, 1869

Rodriguez-Iturbe, I. and Valdés, J. B.: The geomorphologic structure of hydrologic response, *Water Resour. Res.*, 15, 1409–1420, 1979. 1868

The hydrologic response model SEHR-ECHO v1.0

B. Schaefli et al.

Title Page

Abstract

Introduction

Conclusions

References

Tables

Figures

◀

▶

◀

▶

Back

Close

Full Screen / Esc

Printer-friendly Version

Interactive Discussion

- Rodriguez-Iturbe, I., Porporato, A., Ridolfi, L., Isham, V., and Cox, D.: Probabilistic modelling of water balance at a point: the role of climate, soil and vegetation, *P. Roy. Soc. Lond. A-Mat.*, 455, 3789–3805, 1999. 1872
- Rohrer, M. B., Braun, L. N., and Lang, H.: Long-term records of snow cover water equivalent in the Swiss Alps. 2. Simulations, *Nord. Hydrol.*, 25, 65–78, 1994. 1872
- Schaefli, B. and Gupta, H.: Do Nash values have value?, *Hydrol. Process.*, 21, 2075–2080, doi:10.1002/hyp.6825, 2007. 1880
- Schaefli, B. and Huss, M.: Integrating point glacier mass balance observations into hydrologic model identification, *Hydrol. Earth Syst. Sci.*, 15, 1227–1241, doi:10.5194/hess-15-1227-2011, 2011. 1870
- Schaefli, B., Hingray, B., Niggli, M., and Musy, A.: A conceptual glacio-hydrological model for high mountainous catchments, *Hydrol. Earth Syst. Sci.*, 9, 95–109, doi:10.5194/hess-9-95-2005, 2005. 1867, 1868, 1870, 1875, 1883, 1893
- Sivapalan, M., Jothityangkoon, C., and Menabde, M.: Linearity and nonlinearity of basin response as a function of scale: discussion of alternative definitions, *Water Resour. Res.*, 38, 1012, doi:10.1029/2001wr000482, 2002. 1868
- Stahl, K., Moore, R., Shea, J., Hutchinson, D., and Cannon, A.: Coupled modelling of glacier and streamflow response to future climate scenarios, *Water Resour. Res.*, 44, W02422, doi:10.1029/2007WR005956, 2008. 1883
- Swiss Federal Office for Statistics: Geostat – Version 1997, Swiss Spatial Land Use Statistics Database, Bern, Switzerland, 2001. 1879
- SwissTopo: DHM25 – the Digital Height Model of Switzerland, 2005. 1897
- SwissTopo: Vector25 – the Digital Landscape Model of Switzerland, 2008. 1897
- Tague, C. L. and Band, L. E.: Evaluating explicit and implicit routing for watershed hydro-ecological models of forest hydrology at the small catchment scale, *Hydrol. Process.*, 15, 1415–1439, doi:10.1002/hyp.171, 2001. 1867
- Tarboton, D. G.: A new method for the determination of flow directions and upslope areas in grid digital elevation models, *Water Resour. Res.*, 33, 309–319, doi:10.1029/96wr03137, 1997. 1869, 1879, 1897
- Tobin, C., Nicótina, L., Parlange, M. B., Berne, A., and Rinaldo, A.: Improved interpolation of meteorological forcings for hydrologic applications in a Swiss Alpine region, *J. Hydrol.*, 401, 77–89, doi:10.1016/j.jhydrol.2011.02.010, 2011. 1869

The hydrologic response model SEHR-ECHO v1.0

B. Schaefli et al.

Title Page

Abstract

Introduction

Conclusions

References

Tables

Figures

◀

▶

◀

▶

Back

Close

Full Screen / Esc

Printer-friendly Version

Interactive Discussion



- Tobin, C., Rinaldo, A., and Schaefli, B.: Snowfall limit forecasts and hydrological modeling, *J. Hydrometeorol.*, 13, 1507–1519, 2012. 1893
- Tobin, C., Schaefli, B., Nicótina, L., Simoni, S., Barrenetxea, G., Smith, R., Parlange, M., and Rinaldo, A.: Improving the degree-day method for sub-daily melt simulations with physically-based diurnal variations, *Adv. Water Resour.*, 55, 149–164, doi:10.1016/j.advwatres.2012.08.008, 2013. 1868, 1882
- Verbunt, M., Gurtz, J., Jasper, K., Lang, H., Warmerdam, P., and Zappa, M.: The hydrological role of snow and glaciers in alpine river basins and their distributed modeling, *J. Hydrol.*, 282, 36–55, 2003. 1878
- Viviroli, D., Zappa, M., Schwanbeck, J., Gurtz, J., and Weingartner, R.: Continuous simulation for flood estimation in ungauged mesoscale catchments of Switzerland – Part I: Modelling framework and calibration results, *J. Hydrol.*, 377, 191–207, doi:10.1016/j.jhydrol.2009.08.023, 2009. 1867
- Vrugt, J. A., Gupta, H. V., Bouten, W., and Sorooshian, S.: A shuffled complex evolution Metropolis algorithm for optimization and uncertainty assessment of hydrologic models, *Water Resour. Res.*, 39, 1201, doi:10.1029/2002WR001642, 2003. 1877
- Vrugt, J., ter Braak, C., Diks, C., Higdon, D., Robinson, B., and Hyman, J.: Accelerating Markov chain Monte Carlo simulation by differential evolution with self-adaptive randomized subspace sampling, *Int. J. Nonlinear Sci.*, 10, 273–290, 2009. 1877
- Wigmosta, M. S., Vail, L. W., and Lettenmaier, D. P.: A distributed hydrology-vegetation model for complex terrain, *Water Resour. Res.*, 30, 1665–1679, doi:10.1029/94wr00436, 1994. 1867
- Wrede, S., Seibert, J., and Uhlenbrook, S.: Distributed conceptual modelling in a Swedish lowland catchment: a multi-criteria model assessment, *Hydrol. Res.*, 44, 318–333, doi:10.2166/nh.2012.056, 2013. 1867
- Yochum, S. E., Bledsoe, B. P., David, G. C. L., and Wohl, E.: Velocity prediction in high-gradient channels, *J. Hydrol.*, 424–425, 84–98, doi:10.1016/j.jhydrol.2011.12.031, 2012. 1883, 1893

GMDD

7, 1865–1904, 2014

The hydrologic
response model
SEHR-ECHO v1.0

B. Schaefli et al.

Title Page

Abstract

Introduction

Conclusions

References

Tables

Figures

⏪

⏩

◀

▶

Back

Close

Full Screen / Esc

Printer-friendly Version

Interactive Discussion



Table 1. Model parameters describing the physiographic catchment characteristics. The units are given in generic terms (L: length, T: time).

Symbol	Unit	Meaning
A_y	L^2	Source area size
n	–	Number of source areas
l_y	L	Path length
H_y	L a.s.l.	Mean source area elevation

The hydrologic response model SEHR-ECHO v1.0

B. Schaefli et al.

Table 3. The calibrated parameter values corresponding to the parameter set with the best NSE value at the daily time step for the calibration period. The performance criteria values of this set are: $NSE(\text{day, calib}) = 0.82$, $NSE_{\log}(\text{day, calib}) = 0.85$, $\text{bias}(\text{day, calib}) = -0.03$, $NSE(\text{day, valid}) = 0.76$, $NSE_{\log}(\text{day, valid}) = 0.86$, $\text{bias}(\text{day, valid}) = 0.05$, $NSE(\text{hour, valid}) = 0.78$, $NSE_{\log}(\text{hour, valid}) = 0.87$, $\text{bias}(\text{hour, valid}) = -0.12$.

Symbol	Unit	Value
a_s	$\text{mm } ^\circ\text{C}^{-1} \text{d}^{-1}$	2.14
a_i	$\text{mm } ^\circ\text{C}^{-1} \text{d}^{-1}$	6.22
G_{\max}	mmd^{-1}	0.18
Z_r	mm	184.75
L_{\max}	mm h^{-1}	0.12
c	–	5.87
K_{sat}	mm h^{-1}	231.96
s_w	–	0.27
s_m	–	0.77
k_{slow}^{-1}	d	146.87
k_{fast}^{-1}	d	6.5
k_{ice}^{-1}	d	22.3

Title Page

Abstract

Introduction

Conclusions

References

Tables

Figures

◀

▶

◀

▶

Back

Close

Full Screen / Esc

Printer-friendly Version

Interactive Discussion



The hydrologic response model SEHR-ECHO v1.0

B. Schaefli et al.

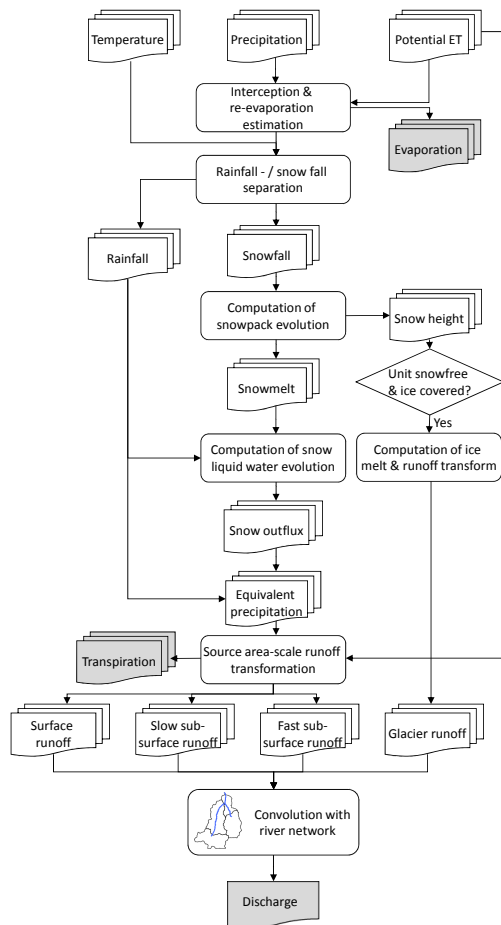


Fig. 1. Flow diagram of the precipitation-discharge computation. The grey boxes highlight the model output time series.

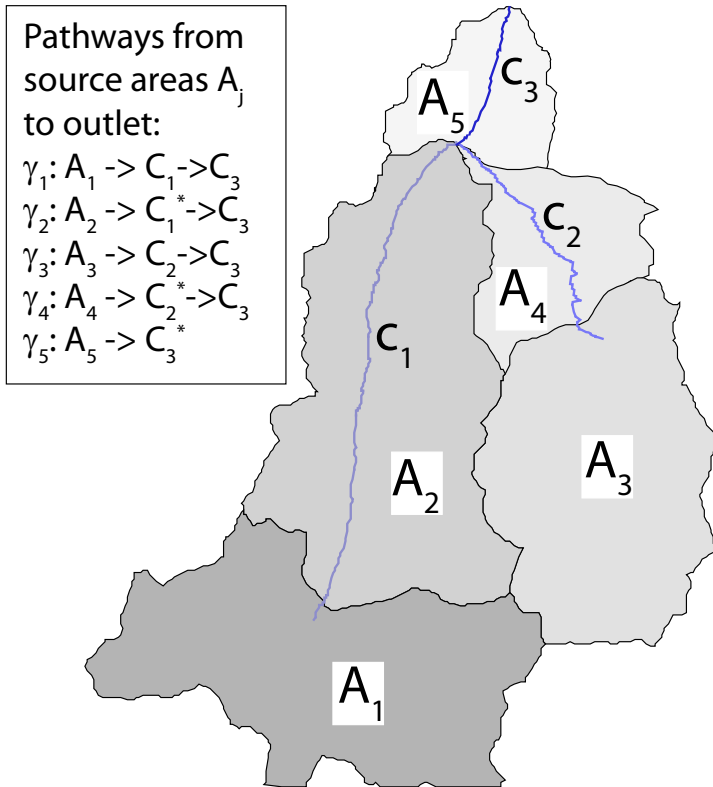


Fig. 2. Sketch of the flow paths from a catchment with five source areas A_j and three channels C_j . The notation C_j^* means that the injection into this channel is not concentrated at the upstream end but, in theory, randomized and integrated over the channel length (Bras and Rodriguez-Iturbe, 1985). In practice, we take half of the channel length.

Title Page

Abstract

Introduction

Conclusions

References

Tables

Figures

⏪

⏩

◀

▶

Back

Close

Full Screen / Esc

Printer-friendly Version

Interactive Discussion



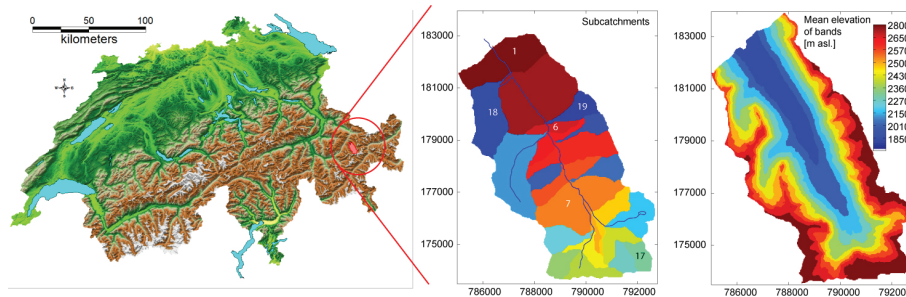


Fig. 3. Location of the Dischmabach catchment within Switzerland (source: SwissTopo, 2008, 2005) and the 23 subcatchments identified with TauDEM Version 5 (Tarboton, 1997). The 10 elevation bands set-up in the right plot is used for comparison purposes in Sect. 5.1. The latitude and longitude are indicated in the Swiss coordinate system (in km).

[Title Page](#)[Abstract](#)[Introduction](#)[Conclusions](#)[References](#)[Tables](#)[Figures](#)[◀](#)[▶](#)[◀](#)[▶](#)[Back](#)[Close](#)[Full Screen / Esc](#)[Printer-friendly Version](#)[Interactive Discussion](#)

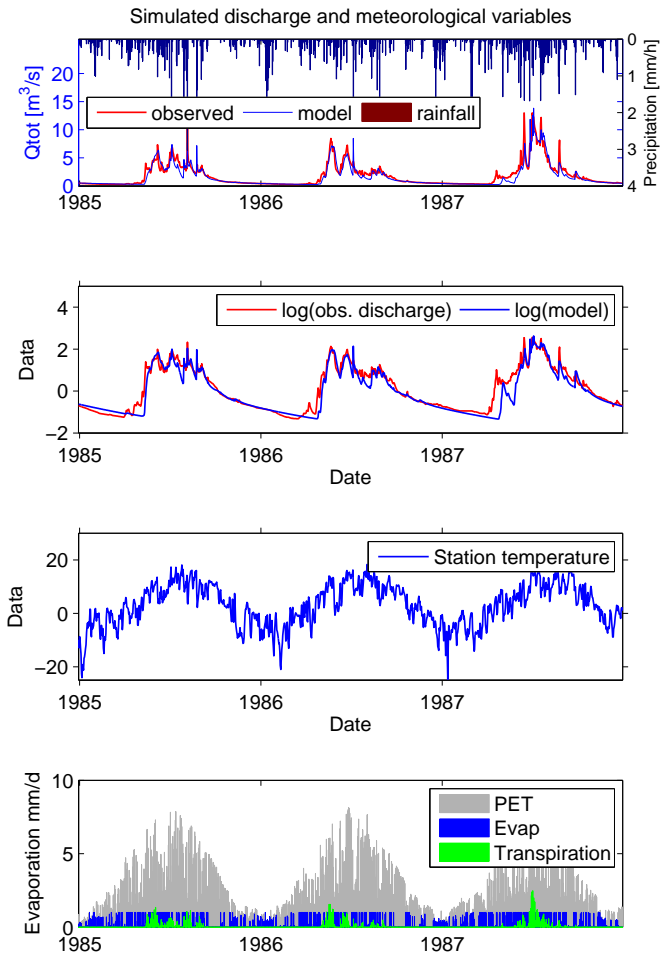


Fig. 4. Observed and simulated hydro-meteorological time series of model state variables for the parameter set of Table 3.

Title Page

Abstract

Introduction

Conclusions

References

Tables

Figures



Back

Close

Full Screen / Esc

Printer-friendly Version

Interactive Discussion



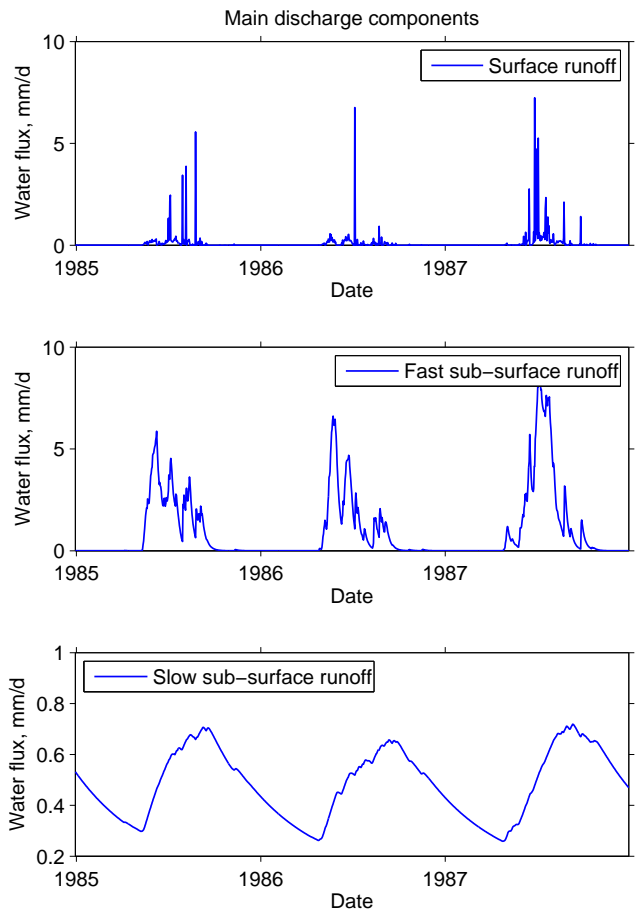


Fig. 5. Time series of the streamflow components (direct surface flow, fast subsurface flow and slow (deep) subsurface flow) corresponding to the parameter set of Table 3 and the discharge plot of Fig. 4.

The hydrologic response model SEHR-ECHO v1.0

B. Schaefli et al.

Best 100 simulations under NSE with daily time step

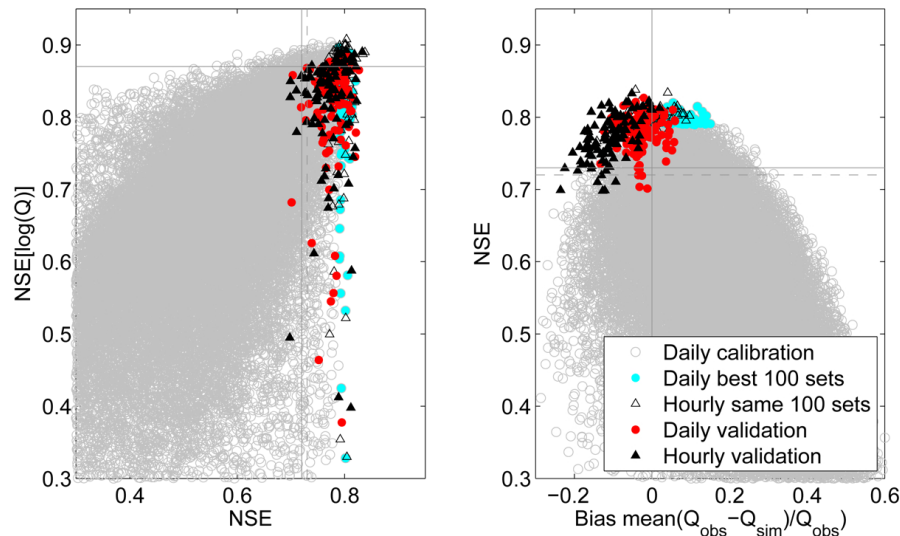


Fig. 6. NSE vs. NSE-log for all simulated parameter sets during model calibration with daily time step (period 1981–1994), values for 100 parameter sets with best NSE values, values for the same parameter sets simulated over validation period (1993–2003) and values for the same parameter sets simulated at hourly time step over the validation period. The lines indicate the benchmark values for daily and hourly (broken line) time steps.

Title Page

Abstract

Introduction

Conclusions

References

Tables

Figures

◀

▶

◀

▶

Back

Close

Full Screen / Esc

Printer-friendly Version

Interactive Discussion



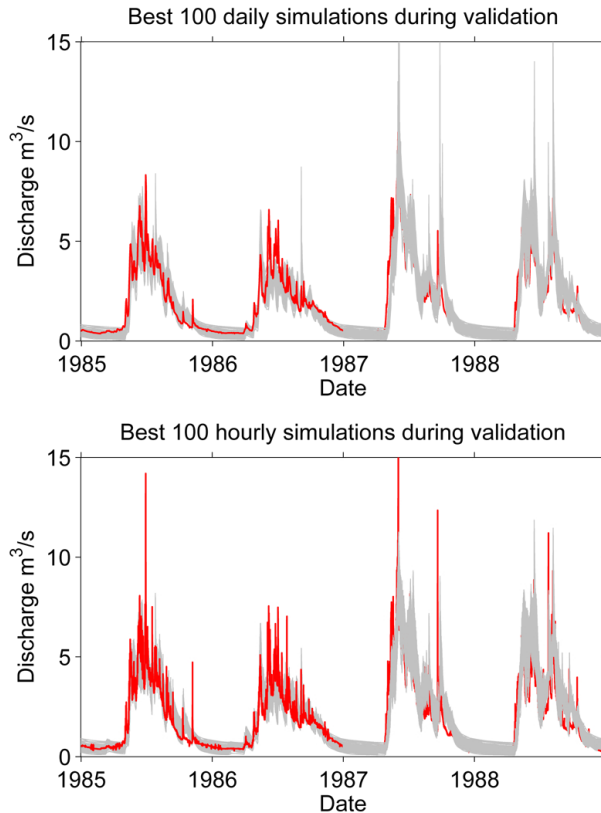


Fig. 7. Predictions resulting from the 100 best parameter sets obtained under NSE for a daily time step (of the total 35 000 Monte Carlo simulations); top: simulation at the daily time step, bottom: simulation at the hourly time step (same parameter sets). The 1st half of the plot shows that the prediction limits are reasonably narrow, the reserved plotting order in the 2nd half shows that the observations are well spanned (79 % (daily) respectively 75 % (hourly) of the observed time steps fall into the range spanned by the simulations).

Title Page

Abstract

Introduction

Conclusions

References

Tables

Figures



Back

Close

Full Screen / Esc

Printer-friendly Version

Interactive Discussion



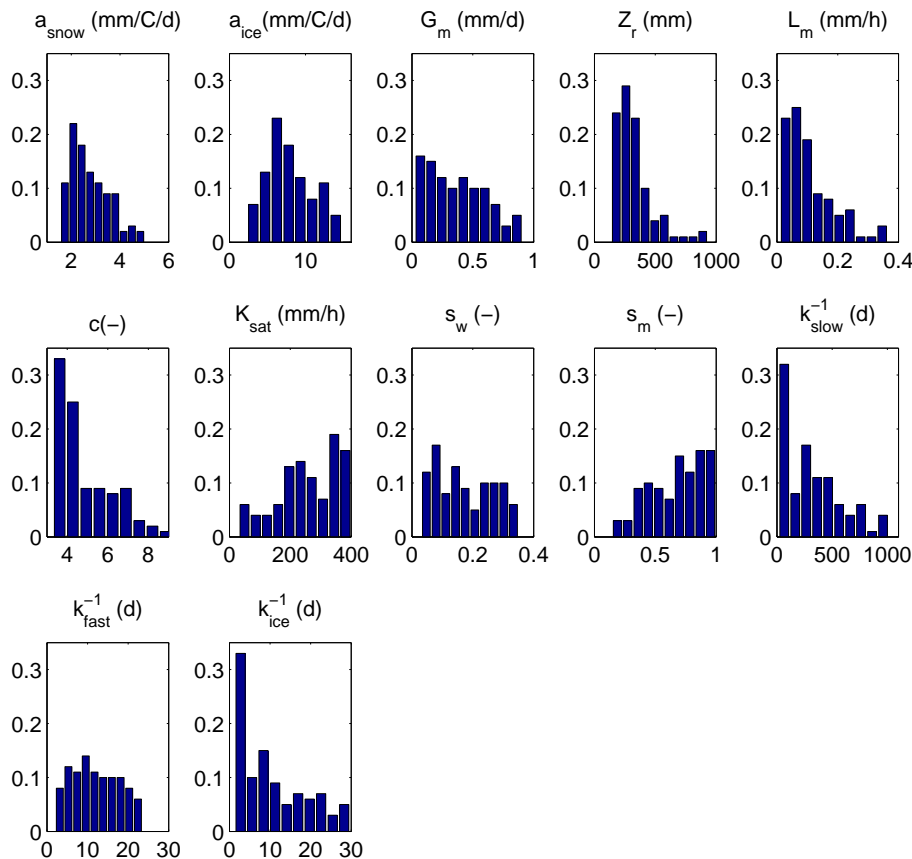


Fig. 8. Parameter distributions obtained for the best 100 parameter sets under NSE at a daily time step; s_m , k_{slow} respectively a_i result from a multiplication of s_w , k_{fast} respectively a_s with the distribution of the corresponding calibrated scaling parameters.

The hydrologic
response model
SEHR-ECHO v1.0

B. Schaefli et al.

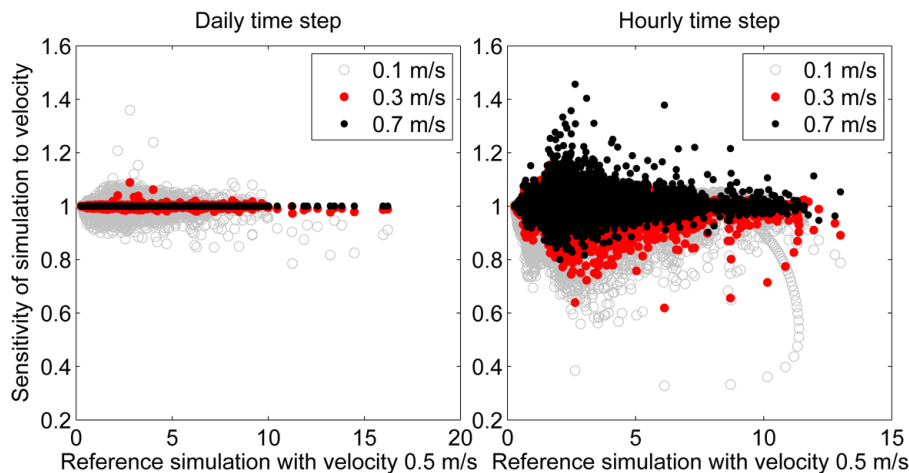


Fig. 9. Sensitivity of the discharge simulation with respect to the in-stream flow velocity plotted against the reference simulation with parameters of Table 3 and velocity of 0.5 m s^{-1} ; the sensitivity is expressed as the relative difference to the reference simulation for each time step.

[Title Page](#)[Abstract](#)[Introduction](#)[Conclusions](#)[References](#)[Tables](#)[Figures](#)[⏪](#)[⏩](#)[◀](#)[▶](#)[Back](#)[Close](#)[Full Screen / Esc](#)[Printer-friendly Version](#)[Interactive Discussion](#)

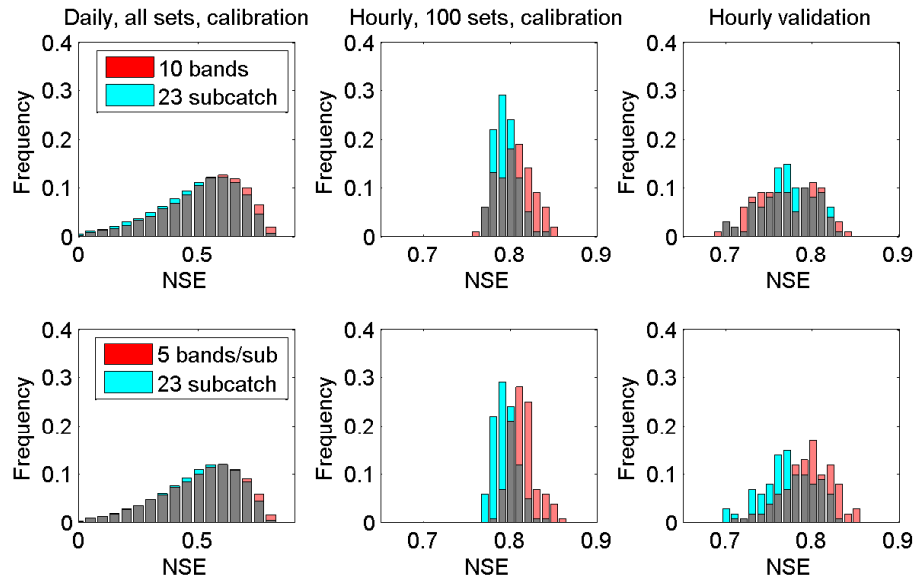


Fig. 10. Comparison of model performance of the subcatchment-based model set-up (23 subcatchments) to elevation band set-ups. Top row: comparison to 10 elevation bands (see Fig. 3), bottom row: comparison to a combination of elevation bands and subcatchments (5 bands for each of the 23 subcatchments). Left column: distribution of the Nash–Sutcliffe (NSE) efficiency computed at a daily time step for the calibration period (shown are parameter sets with $NSE > 0$); center column: NSE distribution of the 100 sets with the highest NSE values at the daily time step run at hourly time step for the calibration period; right column: same 100 sets run at an hourly time step for the validation period. The same 35 000 parameter sets are run for all three model set-ups.

[Title Page](#)
[Abstract](#)
[Introduction](#)
[Conclusions](#)
[References](#)
[Tables](#)
[Figures](#)
[⏪](#)
[⏩](#)
[◀](#)
[▶](#)
[Back](#)
[Close](#)
[Full Screen / Esc](#)
[Printer-friendly Version](#)
[Interactive Discussion](#)
